REMARKS ON HIGH-RESOLUTION NON-OSCILLATORY CENTRAL SCHEMES FOR MULTI-DIMENSIONAL SYSTEMS OF CONSERVATION LAWS. PART I: AN IMPROVED QUADRATURE RULE FOR THE FLUX-COMPUTATION.

KNUT–ANDREAS LIE AND SEBASTIAN NOELLE

ABSTRACT. We present a new second-order, nonoscillatory, central difference scheme on two-dimensional, staggered, Cartesian grids for systems of conservation laws. The scheme uses a new, carefully designed integration rule for the flux computations and thereby takes more propagation directions into account. This effectively reduces grid orientation effects produced for two-dimensional, radially symmetric gas flows.

1. INTRODUCTION

Non-oscillatory, central difference schemes have proved to be efficient computational methods for systems of conservation laws. Since the schemes apply no characteristic information or Riemann solvers, they yield especially compact and simple computer code and can easily be applied to systems for which no Riemann solver exists. Moreover, the schemes are truly multi-dimensional in the sense that they do not use dimensional splitting in any form. We refer the reader to [1, 2, 3, 4] for an introduction to higher-order central schemes and to [5, 6, 7, 8, 9, 10, 11] and references therein for recent related progress.

In this note, which is the first in a series of three (see [12]), we review the two-dimensional extension [3, 4] of the second-order central difference scheme of Nessyahu and Tadmor [1] with special emphasis on the quadrature rules for the fluxes across the boundaries of the cells. We present a radially symmetric explosion problem in gas dynamics for which the scheme clearly produces grid orientation effects. This motivates the derivation of a new central difference scheme that takes more propagation directions into account, which is achieved by introducing a carefully designed integration rule for the flux computations. The new scheme has less grid orientation effects and preserves symmetries better than the original scheme at the expense of a slightly higher runtime. This is demonstrated clearly for our radially symmetric test problem, for which (almost) all directional effects are eliminated.

2. FLUX COMPUTATIONS IN THE TWO-DIMENSIONAL NESSYAHU–TADMOR SCHEME

In this section we review the staggered, second-order, central difference scheme introduced in [3, 4] for systems of hyperbolic conservation laws

$$u_t + f(u)_x + g(u)_y = 0, \tag{1}$$

where $u : \mathbb{R}^2 \times \mathbb{R}_+ \to \mathbb{R}^m$ is the vector of conservative variables, $f, g : \mathbb{R}^m \to \mathbb{R}^m$ are the fluxes in x- and y-direction, and the initial data u_0 are given at time $t = 0$. Prototypes of these equations are the Euler equations of gas dynamics, the shallow water equations, and the equations of ideal magnetohydrodynamics, to name a few.

The idea of using staggered grids goes back to Lax [13] and Friedrichs. Nessyahu and Tadmor [1] extended the one-dimensional, first-order Lax–Friedrichs scheme to second-order accuracy using piecewise linear reconstructions in space and Taylor expansions in time. Arminjon et al. [2, 5, 6] generalized this to two-dimensional *unstructured* grids. In the present note we will build upon a direct extension of the Nessyahu–Tadmor scheme to two-dimensional *Cartesian* grids which was introduced by Arminjon, Stanescu and Viallon [3] and Jiang and Tadmor [4]. We will refer to this scheme by the acronym "NT2d" scheme.

Let us describe the two-dimensional extension NT2d of the Nessyahu–Tadmor scheme: We denote the grid points by $x_j = j\Delta x$, $y_k = k\Delta y$ and $t_n = n\Delta t$, $j, k \in \mathbb{Z}$, $n \in \mathbb{N}$. The NT2d scheme approximates cell-averages of the solution on two sets of grids: At even time-steps t_n, $n = 2p$, the mesh consists of the cells

$$C_{j,k} = [x_{j-\frac{1}{2}}, x_{j+\frac{1}{2}}] \times [y_{k-\frac{1}{2}}, y_{k+\frac{1}{2}}]$$

(we will call these the *original*, or *non-staggered*, cells). At odd time steps t_n, $n = 2p+1$, the cells are

$$C_{j+\frac{1}{2},k+\frac{1}{2}} = [x_j, x_{j+1}] \times [y_k, y_{k+1}]$$

(the *staggered* cells).

Suppose now that the numerical solution at time t_n, n even, is given as a piecewise linear function over the *original* grid,

$$\overline{w}(x,y,t_n) = \overline{w}^{\,n}_{jk} + \frac{x - x_j}{\Delta x} w'_{jk} + \frac{y - y_k}{\Delta y} w^{\backprime}_{jk} \quad \text{for } (x,y) \in C_{jk}. \tag{2}$$

Thus the values $\overline{w}^{\,n}_{jk}$ are the cell-averages, given either by the previous computational step or as the exact cell-average of the initial data for $n = 0$. The finite-difference-operators $' \approx \Delta x \frac{\partial}{\partial_x}$ and $^{\backprime} \approx \Delta y \frac{\partial}{\partial_y}$ are realized by piecewise linear reconstructions with standard limiter-functions, which are applied to the components of the conservative variables and the flux-functions (see for example the central WENO reconstruction (9) below or the MinMod reconstruction in [1, 4]).

Let $w : \mathbb{R}^2 \times [t_n, t_{n+1}) \to \mathbb{R}^m$ be the solution of (1) with initial data $\overline{w}(\cdot, t_n)$ prescribed at time t_n. Then the NT2d scheme computes the update $\overline{w}^{\,n+1}_{j+1/2,k+1/2}$ at time t_{n+1} over the *staggered* cells as

$$\begin{aligned}
\overline{w}^{\,n+1}_{j+\frac{1}{2},k+\frac{1}{2}} =& \frac{1}{4}\big(\overline{w}^{\,n}_{jk} + \overline{w}^{\,n}_{j+1,k} + \overline{w}^{\,n}_{j+1,k+1} + \overline{w}^{\,n}_{j,k+1}\big) \\
&+ \frac{1}{16}\big(w'_{jk} + w'_{j,k+1} - w'_{j+1,k} - w'_{j+1,k+1}\big) \\
&+ \frac{1}{16}\big(w^{\backprime}_{jk} - w^{\backprime}_{j,k+1} + w^{\backprime}_{j+1,k} - w^{\backprime}_{j+1,k+1}\big) \\
&- \frac{\lambda}{2}\Big[f(w^{n+\frac{1}{2}}_{j+1,k}) + f(w^{n+\frac{1}{2}}_{j+1,k+1})\Big] + \frac{\lambda}{2}\Big[f(w^{n+\frac{1}{2}}_{j,k}) + f(w^{n+\frac{1}{2}}_{j,k+1})\Big] \\
&- \frac{\mu}{2}\Big[g(w^{n+\frac{1}{2}}_{j+1,k+1}) + g(w^{n+\frac{1}{2}}_{j,k+1})\Big] + \frac{\mu}{2}\Big[g(w^{n+\frac{1}{2}}_{j+1,k}) + g(w^{n+\frac{1}{2}}_{j,k})\Big],
\end{aligned} \tag{3}$$

where $\lambda = \Delta t/\Delta x$, $\mu = \Delta t/\Delta y$ and

$$w^{n+\frac{1}{2}}_{jk} = \overline{w}^{\,n}_{jk} - \frac{\lambda}{2} f'_{jk} - \frac{\mu}{2} g^{\backprime}_{jk} \tag{4}$$

is a predictor step in the centers of the non-staggered cells at time $t_{n+1/2}$. This predictor step uses the conservation law (1) to approximate the time derivative of w,

$$w_t = -f(w)_x - g(w)_y \approx -\frac{1}{\Delta x} f' - \frac{1}{\Delta y} g^{\backprime}.$$

Given the values $\overline{w}^{n+1}_{j+1/2,k+1/2}$ on the staggered grid, the odd time-step is defined analogously, replacing staggered by non-staggered cells and vice-versa, and this step will produce the cell-averages $\overline{w}^{n+2}_{j,k}$ over the original grid at time t_{n+2}.

Remark 1. *Note that if all approximate derivatives in* (3) *and* (4) *are set to zero, then the scheme coincides with the two-dimensional, first-order Lax–Friedrichs scheme.*

Let us take a closer look at formula (3). The first three lines on the right-hand-side give the cell-average of the reconstruction $\overline{w}(\cdot, t_n)$ in (2) over the staggered cell $C_{j+\frac{1}{2},k+\frac{1}{2}}$. The following two lines approximate the integral of the fluxes across the boundaries of the cell from time t_n to t_{n+1} by a quadrature rule in space-time. Let us write

$$\partial C_{j+\frac{1}{2},k+\frac{1}{2}} \times [t_n, t_{n+1}] = D^{\mathrm{N}}_{j+\frac{1}{2},k+\frac{1}{2}} \cup D^{\mathrm{W}}_{j+\frac{1}{2},k+\frac{1}{2}} \cup D^{\mathrm{S}}_{j+\frac{1}{2},k+\frac{1}{2}} \cup D^{\mathrm{E}}_{j+\frac{1}{2},k+\frac{1}{2}},$$

where the northern, western, southern and eastern sides are

$$\begin{aligned} D^{\mathrm{N}}_{j+\frac{1}{2},k+\frac{1}{2}} &= [x_j, x_{j+1}] \times \{y_{k+1}\} \times [t_n, t_{n+1}], \\ D^{\mathrm{W}}_{j+\frac{1}{2},k+\frac{1}{2}} &= \{x_j\} \times [y_k, y_{k+1}] \times [t_n, t_{n+1}], \\ D^{\mathrm{S}}_{j+\frac{1}{2},k+\frac{1}{2}} &= [x_j, x_{j+1}] \times \{y_k\} \times [t_n, t_{n+1}], \\ D^{\mathrm{E}}_{j+\frac{1}{2},k+\frac{1}{2}} &= \{x_{j+1}\} \times [y_k, y_{k+1}] \times [t_n, t_{n+1}]. \end{aligned}$$

For example, over the western side the space-time quadrature used in (3) is

$$\frac{1}{\Delta y \Delta t} \iint\limits_{D^{\mathrm{W}}_{j+\frac{1}{2},k+\frac{1}{2}}} f(w(x_j, y, t))\, dy\, dt \approx \frac{1}{2}\Big(f\big(w^{n+\frac{1}{2}}_{jk}\big) + f\big(w^{n+\frac{1}{2}}_{jk+1}\big)\Big). \tag{5}$$

The nodes of this quadrature rule are

$$(x_j, y_k, t_{n+1/2}),\ (x_j, y_{k+1}, t_{n+1/2}), \tag{6}$$

see Figure 2(a) on page 6. This is the midpoint rule in time and the trapezoidal rule in space.

Note that for *standard* finite-difference schemes, which do *not* use staggered grids, the reconstruction $\overline{w}(t_n)$ usually has jump-discontinuities at the quadrature points on the interfaces between the cells, and one has to apply Riemann-solvers or artificial viscosity to obtain a stable numerical solution. This complication is completely avoided by the use of *staggered* grids: here the quadrature points lie above the *centers* of the cells of the original grid, where the reconstruction (2) is *smooth.* If we assume that solutions to the conservation law (1) have maximal speeds of propagation $a_{\max}$ and $b_{\max}$ in the x- and y-directions, then the solution of (1) with initial data (2) given at time t_n will remain smooth along $(x_j, y_k) \times [t_n, t_{n+1}]$ as long as the CFL condition

$$\Delta t\ \max\Big(\frac{a_{\max}}{\Delta x}, \frac{b_{\max}}{\Delta y}\Big) < \frac{1}{2} \tag{7}$$

is satisfied. It is therefore justified to approximate the solution at $(x_j, y_k,\ t_{n+1/2})$ using Taylor expansions and the conservation law (1). This is what is done in (4). As a consequence, no characteristic decompositions of the flux-vectors are needed. This is the “truly multi-dimensional” content of the NT2d scheme. It makes the scheme particularly simple to implement and computationally very efficient.

Besides these obvious advantages of the staggered schemes, there are at least three disadvantages known to the authors. First, linear discontinuities are not as sharply resolved as for Riemann-solver based schemes, especially in the one-dimensional stationary case. We will address this issue in the second note in this series of remarks on central difference schemes [12], where we demonstrate that sharp resolution of linear fields can be obtained by including Harten's artificial compression method, i.e., using a partial characteristic decomposition to construct a steeper reconstruction near linear discontinuities. Second, we have observed an instability of the NT2d scheme for a two-dimensional linear advection problem which so far seems to have gone unnoticed in the literature. In the third note in this series [12], we will present and analyze that instability.

In the current note we will concentrate on the multidimensional nature of central schemes, here exemplified through the second-order, staggered NT2d scheme. Although this central difference scheme is multidimensional in the sense that it does not use dimensional splitting or direction-dependent characteristic decompositions, the scheme still exhibits grid orientation effects. This third difficulty will be demonstrated in the following example.

Example 1. Consider the Euler equations of gas dynamics

$$\begin{bmatrix} \rho \\ \rho u \\ \rho v \\ E \end{bmatrix}_t + \begin{bmatrix} \rho \\ \rho u^2 + p \\ \rho uv \\ u(E+p) \end{bmatrix}_x + \begin{bmatrix} \rho v \\ \rho uv \\ \rho v^2 + p \\ v(E+p) \end{bmatrix}_y = 0 \tag{8}$$

for an ideal, polytropic gas with equation of state $E = \rho(u^2+v^2)/2 + p/(\gamma-1)$ and gas constant $\gamma = 1.4$. As initial data, we use a circular variant of Sod's shock tube problem with (ρ, u, v, p) equal to $(1.0, 0, 0, 1.0)$ inside a circle of radius 0.4 and equal to $(0.0125, 0, 0, 0.1)$ outside. The solution consists of a circular shock wave propagating outwards from the origin, followed by a contact discontinuity, and a rarefaction wave travelling towards the origin.

To limit numerical derivatives (as in the reconstruction (2)) we use the smooth WENO limiter [14]

$$\mathrm{WENO}(a, b) = \big(w(a)\cdot a + w(b)\cdot b\big)/\big(w(a) + w(b)\big), \tag{9}$$

where the weights are given by $w(a) = \big(\varepsilon + a^2\big)^{-2}$, and $\varepsilon = 10^{-6}$. For instance, for (2), this means that

$$w'_{j,k} = \mathrm{WENO}\big((\overline{w}^{\,n}_{j,k} - \overline{w}^{\,n}_{j-1,k}), (\overline{w}^{\,n}_{j+1,k} - \overline{w}^{\,n}_{j,k})\big).$$

Figure 1 shows a scatter plot of the solution at time $t = 0.2$ computed by the original NT2d scheme. In the current setting, a scatter plot for a given physical quantity is a plot of the value in each grid cell versus the distance of the cell center from the origin. In this way we can present the spread in the data, as a solution with perfect radial symmetry would consist of points lying on a single line.

Although the scheme gives relatively sharp resolution of the shock and the rarefaction wave (the shock width is 1–2 computational cells for each one-dimensional cross-section of the numerical solution), it suffers from grid orientation effects. This is particularly evident for the internal energy in the zone between the shock and the contact discontinuity. Moreover, overshoots are observed in the pressure and radial velocity behind the leading shock in regions close to the diagonal lines $x = \pm y$.

3. An Improved Quadrature Rule

The presence of grid orientation effects observed in computations on radially symmetric solutions, as for instance in Example 1 above for the Euler equations, motivated us to look for a modification for the NT2d scheme that would reduce these directional effects.

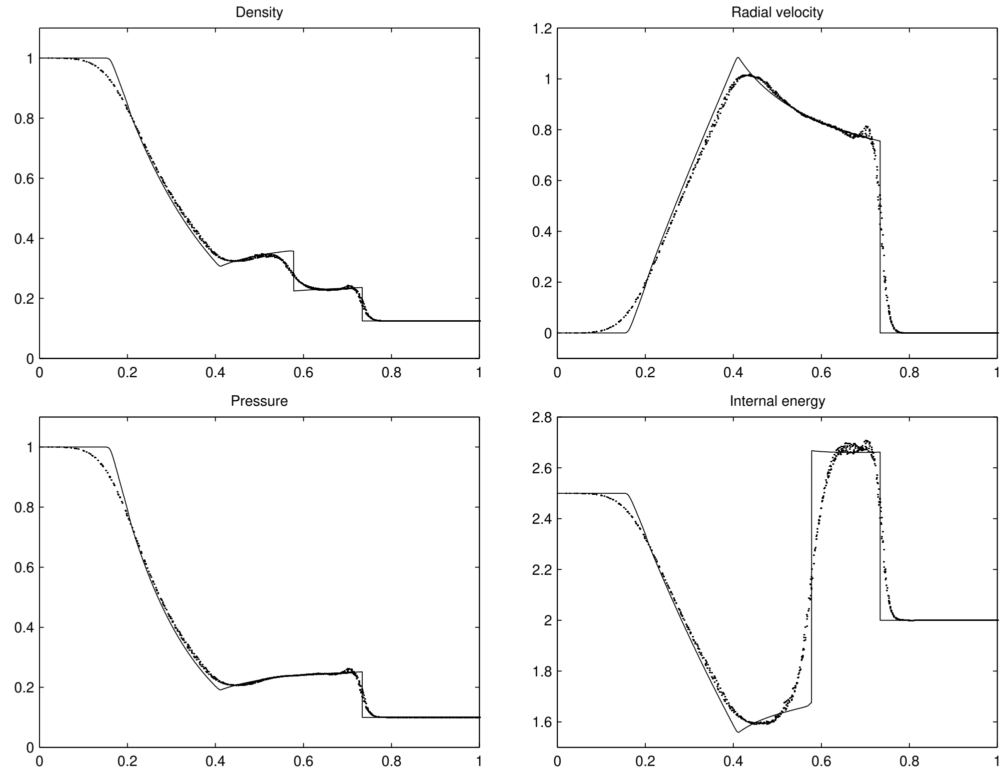

FIGURE 1. Scatter plot of solution at time $t = 0.2$ of the cylindrical explosion problem computed by the original NT2d scheme on a 101×101 grid with WENO limiter and CFL number 0.475.

Here is our new scheme: We propose to replace (3) by

$$
\begin{aligned}
\overline{w}^{\,n+1}_{j+\frac{1}{2},k+\frac{1}{2}} =& \frac{1}{4}\left(\overline{w}^{\,n}_{jk} + \overline{w}^{\,n}_{j+1,k} + \overline{w}^{\,n}_{j+1,k+1} + \overline{w}^{\,n}_{j,k+1}\right) \\
&+ \frac{1}{16}\left(w'_{jk} + w'_{j,k+1} - w'_{j+1,k} - w'_{j+1,k+1}\right) \\
&+ \frac{1}{16}\left(w^{\backprime}_{jk} - w^{\backprime}_{j,k+1} + w^{\backprime}_{j+1,k} - w^{\backprime}_{j+1,k+1}\right) \\
&- \frac{\lambda}{4}\Big[f(w^{n+1}_{j+1,k}) + f^{n,-}_{j+1,k+\frac{1}{2}} + f^{n,+}_{j+1,k+\frac{1}{2}} + f(w^{n+1}_{j+1,k+1})\Big] \\
&+ \frac{\lambda}{4}\Big[f(w^{n+1}_{jk}) + f^{n,-}_{j,k+\frac{1}{2}} + f^{n,+}_{j,k+\frac{1}{2}} + f(w^{n+1}_{j,k+1})\Big] \\
&- \frac{\mu}{4}\Big[g(w^{n+1}_{j,k+1}) + g^{n,-}_{j+\frac{1}{2},k+1} + g^{n,+}_{j+\frac{1}{2},k+1} + g(w^{n+1}_{j+1,k+1})\Big] \\
&+ \frac{\mu}{4}\Big[g(w^{n+1}_{jk}) + g^{n,-}_{j+\frac{1}{2},k} + g^{n,+}_{j+\frac{1}{2},k} + g(w^{n+1}_{j+1,k})\Big],
\end{aligned} \tag{10}
$$

where

$$
w^{n+1}_{jk} = \overline{w}^{\,n}_{jk} - \lambda f'_{jk} - \mu g^{\backprime}_{jk} \tag{11}
$$

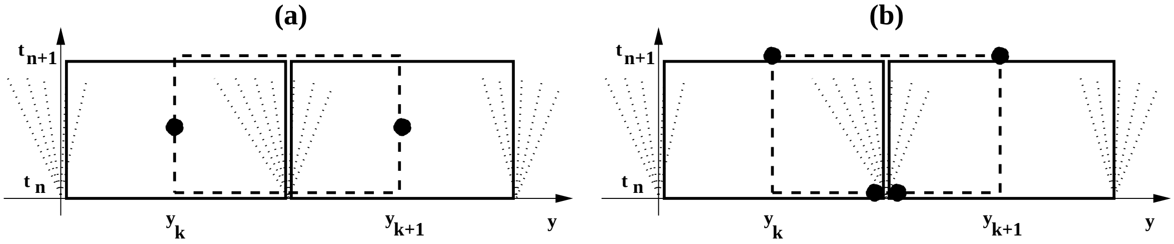

FIGURE 2. Quadrature points for the fluxes over the western side $D^{\mathrm{W}}_{j+1/2,k+1/2}$ of the staggered grid, shown in the (y,t)-plane. The dashed rectangle is $D^{\mathrm{W}}_{j+1/2,k+1/2}$ and the solid rectangles are the sides $D^{\mathrm{W}}_{j,k}$ and $D^{\mathrm{W}}_{j,k+1}$ of the original grid. The dotted lines symbolize the Riemann-fan originating from the cell-boundaries of the original grid. (a) NT2d scheme. (b) Our new scheme.

and

$$
\begin{aligned}
f^{n,-}_{j,k+\frac{1}{2}} &= f(\overline{w}^{\,n}_{jk} + \frac{1}{2} w^{\backprime}_{jk}),\\
f^{n,+}_{j,k+\frac{1}{2}} &= f(\overline{w}^{\,n}_{j,k+1} - \frac{1}{2} w^{\backprime}_{j,k+1}),\\
g^{n,-}_{j+\frac{1}{2},k} &= g(\overline{w}^{\,n}_{jk} + \frac{1}{2} w'_{jk}),\\
g^{n,+}_{j+\frac{1}{2},k} &= g(\overline{w}^{\,n}_{j+1,k} - \frac{1}{2} w'_{j+1,k}).
\end{aligned}
\tag{12}
$$

The difference between our new scheme (10)–(12) and the NT2d scheme (3)–(4) is a new quadrature rule in the computation of the fluxes across the sides. For example, the quadrature rule for the western side corresponding to (5) is now

$$
\frac{1}{\Delta y \Delta t} \iint\limits_{D^{\mathrm{W}}_{j+\frac{1}{2},k+\frac{1}{2}}} f(w(x_j,y,t))\,dy\,dt \approx \frac{1}{4}\Big(f\big(w^{n,-}_{j,k+\frac{1}{2}}\big) + f\big(w^{n,+}_{j,k+\frac{1}{2}}\big) + f\big(w^{n+1}_{jk}\big) + f\big(w^{n+1}_{jk+1}\big)\Big). \tag{13}
$$

The nodes of this quadrature rule are

$$
(x_j, y_{k+\frac{1}{2}}, t_n) \tag{14}
$$

at time t_n and

$$
(x_j, y_k, t_{n+1}),\ (x_j, y_{k+1}, t_{n+1}) \tag{15}
$$

at time t_{n+1}, see Figure 2(b).

At the first quadrature point (14) the reconstruction $\overline{w}(\cdot, t_n)$ is now *discontinuous*, so we have to evaluate the fluxes at the *one-sided* limits as in (12).

As long as the CFL condition (7) is satisfied, the quadrature points (15) at time t_{n+1} still lie within the domain of smoothness of the solution to (1) with initial data (2). Therefore it is justified to extrapolate the solution using Taylor series. This is done in (11).

The main advantage of the new quadrature is that it takes *more directions* into account. To see this, let us have a look at the “floorplan” of the two schemes in Figure 3. The NT2d scheme evaluates all fluxes at the corners of the staggered cell. If we multiply (3) by $\Delta x \Delta y / \Delta t$ and collect the fluxes at the quadrature point $(x_{j+1}, y_{k+1}, t_{n+1/2})$ (the north-east

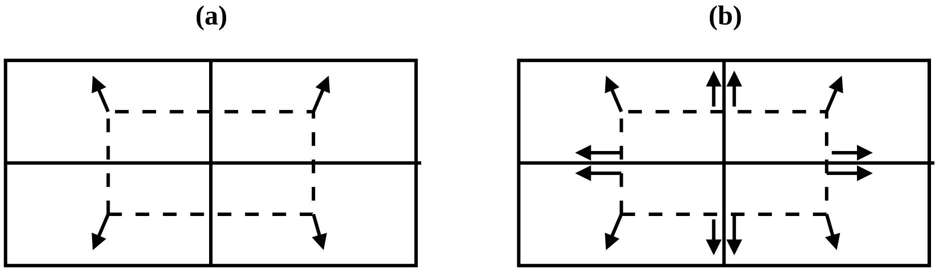

FIGURE 3. Floor-plan of the staggered schemes in the (x, y)-plane. The solid lines symbolize the original cells C_{jk}, the dashed line the staggered cell $C_{j+\frac{1}{2},k+\frac{1}{2}}$, and the arrows the fluxes across its boundaries. (a) NT2d scheme. (b) Our new scheme.

corner), we obtain a contribution of

$$\frac{\Delta y}{2} f(w^{n+\frac{1}{2}}_{j+1,k+1}) + \frac{\Delta x}{2} g(w^{n+\frac{1}{2}}_{j+1,k+1})$$

to the flux across the boundary of the cell. This adds up to evaluating the normal flux in the direction

$$n_{\mathrm{NE}} = (\Delta y, \Delta x)/(\Delta x^2 + \Delta y^2)^{\frac{1}{2}}.$$

At the north-west, south-west and south-east corners we have the directions

$$\begin{aligned} n_{\mathrm{NW}} &= (-\Delta y, \Delta x)/(\Delta x^2 + \Delta y^2)^{\frac{1}{2}}, \\ n_{\mathrm{SW}} &= (-\Delta y, -\Delta x)/(\Delta x^2 + \Delta y^2)^{\frac{1}{2}}, \\ n_{\mathrm{SE}} &= (\Delta y, -\Delta x)/(\Delta x^2 + \Delta y^2)^{\frac{1}{2}}. \end{aligned}$$

For a square grid, these are the diagonal directions, and for a general Cartesian grid, the directions normal to the diagonal directions, see Figure 3(a). This leads us to a reinterpretation of the NT2d scheme: rather than evaluating fluxes across the *sides* of the staggered cells, it computes fluxes across its *corners*. The grid directions themselves are not taken into account.

The new scheme (10) uses two sets of quadrature points, those at the old time t_n in the centers of the sides, see (14), and those at time t_{n+1} in the corners, see (15). Therefore we have now eight directions in two space-dimensions instead of four for the NT2d scheme, see Figure 3(b). As we shall show below, this does reduce grid orientation effects for the radially symmetric flow in Example 1.

To obtain more propagation directions, we must pay the price of more flux evaluations, thus making the scheme computationally more expensive. When implemented directly as in (10), twelve flux-evaluations are needed to update a cell instead of four for the NT2d scheme. However, the additional flux-evaluations can be completely avoided by setting

$$\begin{aligned} f^{n,-}_{j,k+\frac{1}{2}} &= f(\overline{w}^{\,n}_{jk}) + \frac{1}{2} f^{\backprime}_{jk} \\ f^{n,+}_{j,k+\frac{1}{2}} &= f(\overline{w}^{\,n}_{j,k+1}) - \frac{1}{2} f^{\backprime}_{j,k+1} \\ g^{n,-}_{j+\frac{1}{2},k} &= g(\overline{w}^{\,n}_{jk}) + \frac{1}{2} g'_{jk} \\ g^{n,+}_{j+\frac{1}{2},k} &= g(\overline{w}^{\,n}_{j+1,k}) - \frac{1}{2} g'_{j+1,k} \end{aligned} \tag{16}$$

which is exact for linear flux functions. Therefore all additional work we need to do is to compute $f^{\backslash}$ and g' at time t_n at the centers of the original cells C_{jk}. In our test calculations, we always use the scheme (10), (11) and (16), and call this "our new scheme".

Similarly as in [4, Theorem 1], we can prove the following local maximum principle for our new scheme:

Theorem 1. *Consider the scheme (10), (11) and (16) together with the following definition of the discrete derivatives:*

$$w'_{jk} = MM\Big\{\theta(\overline{w}^n{}_{j+1,k} - \overline{w}^n_{j,k}), \frac{1}{2}(\overline{w}^n_{j+1,k} - \overline{w}^n_{j-1,k}), \theta(\overline{w}^n_{j,k} - \overline{w}^n_{j-1,k})\Big\}$$
$$w^{\backslash}_{jk} = MM\Big\{\theta(\overline{w}^n_{j,k+1} - \overline{w}^n_{j,k}), \frac{1}{2}(\overline{w}^n_{j,k+1} - \overline{w}^n_{j,k-1}), \theta(\overline{w}^n_{j,k} - \overline{w}^n_{j,k-1})\Big\}$$
$$f'_{jk} = MM\Big\{\theta(f(\overline{w}^n_{j+1,k}) - f(\overline{w}^n_{j,k})), \frac{1}{2}(f(\overline{w}^n_{j+1,k}) - f(\overline{w}^n_{j-1,k})), \theta(f(\overline{w}^n_{j,k}) - f(\overline{w}^n_{j-1,k}))\Big\}$$
$$f^{\backslash}_{jk} = MM\Big\{\theta(f(\overline{w}^n_{j,k+1}) - f(\overline{w}^n_{j,k})), \frac{1}{2}(f(\overline{w}^n_{j,k+1}) - f(\overline{w}^n_{j,k-1})), \theta(f(\overline{w}^n_{j,k}) - f(\overline{w}^n_{j,k-1}))\Big\}$$
$$g'_{jk} = MM\Big\{\theta(g(\overline{w}^n_{j+1,k}) - g(\overline{w}^n_{j,k})), \frac{1}{2}(g(\overline{w}^n_{j+1,k}) - g(\overline{w}^n_{j-1,k})), \theta(g(\overline{w}^n_{j,k}) - g(\overline{w}^n_{j-1,k}))\Big\}$$
$$g^{\backslash}_{jk} = MM\Big\{\theta(g(\overline{w}^n_{j,k+1}) - g(\overline{w}^n_{j,k})), \frac{1}{2}(g(\overline{w}^n_{j,k+1}) - g(\overline{w}^n_{j,k-1})), \theta(g(\overline{w}^n_{j,k}) - g(\overline{w}^n_{j,k-1}))\Big\}$$

where $\theta \in [1, 2)$ *and*

$$MM\{v_1, v_2, \dots\} = \begin{cases} \min_p\{v_p\} & \text{if} \quad v_p > 0 \quad \forall p, \\ \max_p\{v_p\} & \text{if} \quad v_p < 0 \quad \forall p, \\ 0 & \text{otherwise.} \end{cases}$$

Suppose that the CFL-condition

$$\Delta t \ \max\Big(\frac{a_{\max}}{\Delta x}, \frac{b_{\max}}{\Delta y}\Big) \le C_\theta \tag{17}$$

holds, where the CFL-number C_θ *is given by*

$$C_\theta = -\frac{2+\theta}{6\,\theta} + \sqrt{\Big(\frac{2+\theta}{6\,\theta}\Big)^2 + \frac{2-\theta}{12\,\theta}}. \tag{18}$$

Then the update $\overline{w}^{n+1}_{j+\frac{1}{2},k+\frac{1}{2}}$ *satisfies the local maximum principle*

$$\min_{j',k'=0,1} \overline{w}^n_{j+j',k+k'} \le \overline{w}^{n+1}_{j+\frac{1}{2},k+\frac{1}{2}} \le \max_{j',k'=0,1} \overline{w}^n_{j+j',k+k'}. \tag{19}$$

Remark 2. *(a) The proof is very similar to the one of* [4, Theorem 1]*, and we omit it.*

(b) Our CFL-condition (18) is slightly more restrictive than the one in [4]*. For example, for* $\theta = 1$ *we obtain* $C_1 = 1/\sqrt{3} - 1/2 \approx 0.077$*, as opposed to* $C_1 = (\sqrt{7} - 2)/6 \approx 0.1076$ *for the NT2d scheme. For* $\theta = 2$*,* $C_2 = 0$*, as in* [4]*.*

Example 1 revisited. Let us revisit the radially symmetric Sod problem discussed above and recompute the approximate solution using our new scheme with exactly the same parameters as in Figure 1. Figure 4 shows a scatter plot of the corresponding solution at time $t = 0.2$. Now, most of the directional effects have disappeared, in particular the overshoots in pressure and radial velocity immediately behind the leading shock.

Table 1 gives L^1 errors and runtimes for the two computations. The runtimes are measured on a 300 MHz Pentium processor and the errors are computed relative to the cell average

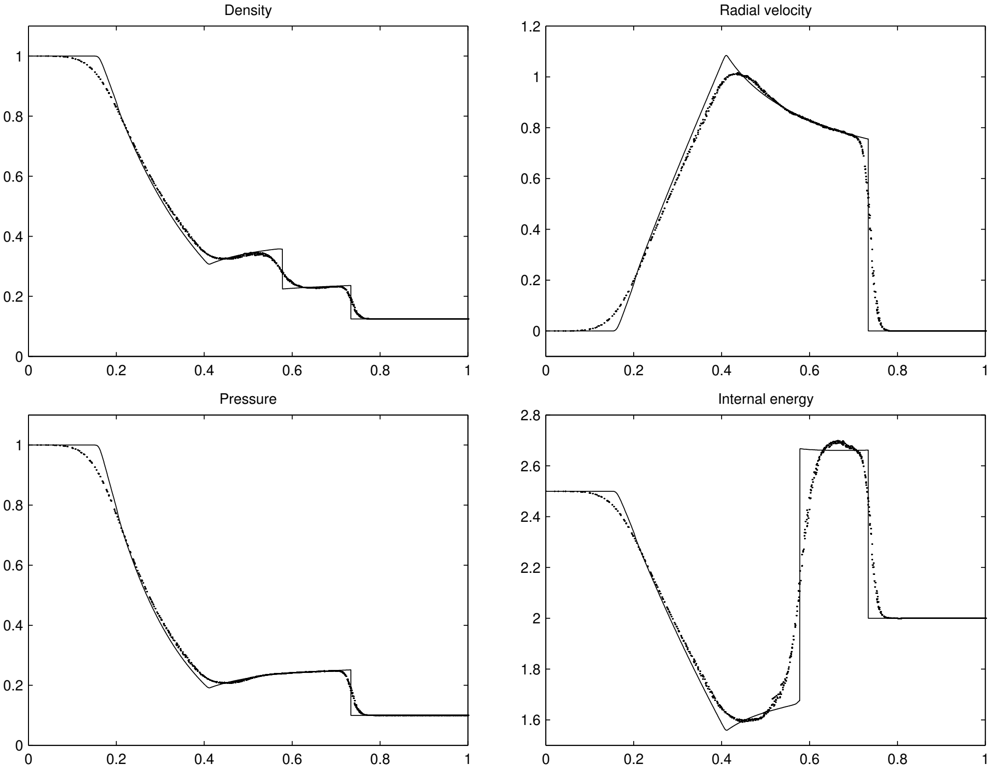

FIGURE 4. Scatter plot of solution at time $t = 0.2$ of the cylindrical explosion problem computed by our new scheme on a 101×101 grid with WENO limiter and CFL number 0.475.

TABLE 1. *Runtime and L^1 errors for various quantities for the runs corresponding to Figures 1 and 4.*

	ρ	ρu_r	E	p	u_r	CPU
Figure 1	2.391e-02	1.857e-02	4.450e-02	4.854e-02	1.804e-02	6.0
Figure 4	2.313e-02	1.725e-02	4.179e-02	4.683e-02	1.715e-02	9.2

projection of an accurate front tracking solution [15, § 2.4] of the corresponding reduced one-dimensional, inhomogeneous problem. The improved flux quadrature gives a slight decrease in the error in both primitive and conserved quantities, but raises the computational time by around 50 %. Similar numbers were confirmed for other choices of parameters.

Remark 3. *We have made similar observations for a whole series of radial Riemann problems of the above form (i.e., for varying ρ and p): inclusion of extra propagation directions reduces directional effects.*

Remark 4. *For the opposite problem—a shock-focusing problem with the inner and outer values of p and ρ from Example 1 exchanged—we observed grid-orientation effects near the origin due to the singularity created as the inward propagating shock wave collapses at that point (compare also* [16] *for a discussion of that difficulty). In this case, we were able to eliminate the grid orientation effects by* not limiting the velocity components. *Unfortunately, this is a dangerous technique that hardly would be recommendable for other problems.*

Remark 5. *As is evident from Figures 1 and 4, the linear discontinuities are poorly resolved by both central schemes. To compensate for this well-known weakness, one can introduce an* artificial compression method *(ACM). This will be done in the second note in this series, where we will also return to a more thorough discussion of the current example (see* [12]*).*

4. Concluding Remarks

We have demonstrated how one can increase the number of propagation directions in a two-dimensional central difference scheme by a careful design of the quadrature rule used in the numerical flux computation. The improved performance of our new central scheme is particularly visible for radially symmetric problems with strong shocks. For other problems, its advantages may be less evident. Still, it could be worthwhile to use the new quadrature rule even in these cases as a means of reducing grid orientation effects, since this will increase the runtime only slightly.

References

[1] H. Nessyahuh and E. Tadmor. Non-oscillatory central differencing for hyperbolic conservation laws. *J. Comput. Phys.* 87:408–463, 1990.

[2] P. Arminjon and M.-C. Viallon. Généralisation du schéma de Nessyahu–Tadmor pour une équation hyperbolique à deux dimensions d'espace. *C.R. Acad. Sci. Paris*, 320(série I):85–88, 1995.

[3] P. Arminjon, D. Stanescu and M.-C. Viallon. A two-dimensional finite volume extension of the Lax–Friedrichs and Nessyahu-Tadmor schemes for compressible flows. *Proc. 6th. Int. Symp. on CFD, Lake Tahoe* M. Hafez and K. Oshima (eds.) , Vol. IV, pp. 7–14, 1995.

[4] G.-S. Jiang and E. Tadmor. Nonoscillatory central schemes for multidimensional hyperbolic conservation laws. *SIAM J. Sci. Comput.* 19(6):1892–1917 (electronic), 1998.

[5] P. Arminjon, M.-C. Viallon and A. Madrane. A finite volume extension of the Lax–Friedrichs and Nessyahu-Tadmor schemes for conservation laws on unstructured grids. *Int. J. Comput. Fluid Dyn.* 9(1):1–22, 1997.

[6] P. Arminjon and M.-C. Viallon. Convergence of a finite volume extension of the Nessyahu–Tadmor scheme on unstructured grids for a two-dimensional linear hyperbolic equation. *SIAM J. Numer. Anal.* 36(3):738–771, 1999.

[7] X.-D. Liu and E. Tadmor. Third order nonoscillatory central scheme for hyperbolic conservation laws. *Numer. Math.* 79:397–425, 1998.

[8] A. Kurganov and E. Tadmor. New high-resolution central schemes for nonlinear conservation laws and convection-diffusion equations. *Preprint* 1999 (to appear in *J. Comput. Phys*).

[9] D. Levy, G. Puppo, G. Russo. Compact central WENO schemes for multidimensional conservation laws. *Preprint* 1999 (LBLN-43961).

[10] A. Kurganov, S. Noelle and G. Petrova. Semi-discrete central-upwind schemes for hyperbolic conservation laws and Hamilton-Jacobi equations. *Preprint* 2000 (to be submitted).

[11] Y. C. Tai, S. Noelle, N. Gray and K. Hutter. Shock capturing and front tracking methods for granular avalanches. *Preprint* 2000 (to be submitted to *J. Comput. Phys*).

[12] K.-A. Lie and S. Noelle. Remarks on high-resolution non-oscillatory central schemes for multi-dimensional systems of conservation laws. Part II: Artificial compression. Part III: Stability. *Preprints* 2000 (to be submitted).

[13] P. Lax. Weak solutions of nonlinear hyperbolic equations and their numerical computation. *Comm. Pure Appl. Math.* 7:159–193, 1954.

[14] G.-S. Jiang and C.-W. Shu. Efficient implementation of weighted ENO schemes. *J. Comput. Phys.* 26:202–228, 1996.

[15] R. Holdahl, H. Holden, and K.-A. Lie. Unconditionally stable splitting methods for the shallow water equations. *BIT*, 39(3):451–472, 1999.

[16] A.-T. Morel, M. Fey and J. Maurer. Multidimensional high-order method of transport for the shallow water equations. In *Proceedings of the ECCOMAS 96 Conference*, Paris, John Wiley & Sons, 1996.

(Knut–Andreas Lie)
SINTEF Applied Mathematics,
P.0. Box 124 Blindern, N–0314 Oslo, Norway
Also: Department of Informatics, University of Oslo
E-mail address: Knut-Andreas.Lie@math.sintef.no
URL: http://www.ifi.uio.no/~kalie/

(Sebastian Noelle)
Institute of Applied Mathematics, Bonn University,
Wegelerstr. 10, 53115 Bonn, Germany
E-mail address: noelle@iam.uni-bonn.de
URL: http://www-mathphys.iam.uni-bonn.de/~noelle/